

An Investigation and Evaluation of VVT/VVA Strategies in a Diesel HCCI Engine using 3D CFD

Zhijun Peng

Department of Engineering and Design, University of Sussex, UK

Ming Jia

School of Energy and Power Engineering, Dalian University of Technology, People's Republic of China

ABSTRACT

A three-dimensional CFD modeling was carried out to investigate effects of VVT/VVA on gas exchange and fuel-air mixing processes in a diesel HCCI engine with early fuel injection. Four VVT/VVA strategies were conducted for this study: i) NVO strategy with fixed EVO and IVC timings but variable valve lifts – referred as NVO Strategy; ii) NVO strategy with fixed valve profiles but variable EVO and IVC timings – referred as EVO Strategy; iii) NVO strategy with fixed valve lifts and fixed EVO and IVC timings but variable EVO and IVC timings – referred as EVC Strategy; iv) VVA with just variable valve lifts – referred as VMAX Strategy. The results indicate that suitable NVO settings will enhance in-cylinder tumble and then increase turbulence intensity before compression-end, though the increased NVO has a negative contribution to swirl ratio. It was found that reducing valve lifts alone is not an efficient way to retain the residual gas, but the function of reduced valve lifts will become significantly obvious by combining it with increasing NVO. For the effect of NVO on in-cylinder temperature, longer NVO will not only increase in-cylinder temperature due to higher residual gas rate, but also improve the in-cylinder temperature homogeneity. Lowering the maximum valve lift or increasing NVO, the unmixed region of in-cylinder charge shrinks. The rich fuel region expands because of the high intake velocity and enhanced turbulence intensity. This is beneficial to the forming of global homogeneous charge. It has been noted from the current study, as the droplet distribution may be influenced more by the in-cylinder air motion caused by NVO when the average droplet size is smaller, it is recommended that future studies explore the effects of VVT/VVA on diesel HCCI mixing and combustion with various advanced fuel injection strategies.

Keywords: HCCI combustion, diesel engine, VVT, VVA, NVO, CFD, KIVA-3V

1 INTRODUCTION

As HCCI (Homogeneous Charge Compression Ignition) combustion continues its long evolution from the research laboratory to the production line, the inherently difficult and sensitive combustion control is the major challenger because ignition timing can not be directly controlled as is the case in conventional internal combustion engines which have fuel injection or spark ignition to determine the ignition timing [1]. Therefore, ensuring that combustion occurs with acceptable timing is totally different from, and is more complicated than, in the case of either SI (Spark Ignition) engine or diesel engine combustion, particularly under transient operating conditions. Because combustion phasing in HCCI combustion is dominated by chemical kinetics [2], which mainly depends on in-cylinder temperature, pressure and charge compositions, there are some special difficulties for developing practical control models of HCCI engines.

Various control strategies, such as variable compression ratio [3], dual-fuel [4, 5] and VVT/VVA (Variable Valve Timing/Actuation), have been investigated by many researchers for controlling HCCI combustion. Adjusting the residual gas fraction by VVT/VVA is considered to be the most promising and feasible way for achieving the HCCI combustion control [6]. There is a multitude of VVT/VVA systems under development, including exhaust re-induction using late IVO (Intake Valve Opening) and late EVC (Exhaust Valve Closing) [7], exhaust re-breathing using a second exhaust valve event during the intake stroke [8, 9], in-cylinder air out-flowing by late IVC (Intake Valve Closing) [9, 10] and exhaust retention using early EVC and late IVO (also referred as NVO - Negative Valve Overlap) [11, 12].

Caton et al. [13] compared different valve profiles by which exhaust residual may be used to achieve HCCI, and concluded that re-induction strategies by late IVO and late EVC had significant higher efficiencies and reduced NO_x emissions than exhaust retention strategies by NVO, although the fore strategy suffered from higher HC emissions. They also indicated that the best combination of load range, efficiency, and low emissions may be achieved using a re-induction strategy with variable intake lift instead of VVT.

Although the use of VVT/VVA systems in gasoline engines to improve performance has occurred for many years and is well understood, the control of the intake and exhaust valves under firing conditions in diesel engines is relative new [14]. Depending upon the design, VVT/VVA systems have the potential for the performance and control enhancements in diesel engines, such as improved cold-starting, variable swirl ratio and engine braking etc. The VVA/VVT systems allow adequate flexibility in valve actuation to optimize cylinder charging and low-end torque with simultaneous improvements in fuel consumption and drivability [15]. Murata et al. [10] demonstrated that ignition timing control of premixed diesel combustion can be realised by optimizing compressed gas temperature by adopting late IVC. At high-speed and intermediate load operation, Nevin et al. [16] also indicated that the use of late IVC could enable 70% NO_x reduction while maintaining PM levels.

Helmantel and Denbratt [9] re-inducted the exhaust gas from the exhaust port by using a second exhaust valve opening during the intake stroke, and found that it was an efficient way to serve as EGR (Exhaust Gas Recirculation) for controlling the combustion phase. However, the ringing intensity was found to be increased, which is thought to be result of temperature stratification in the trapped cylinder charge. Full-load HCCI operation was tested in a heavy-duty diesel engine equipped with VVT/VVA system by Kodama et al. [17], they indicated that about 50 °CA early IVC or late IVC was required for achieving full-load operation for diesel HCCI engines, and IVC timing should be controlled according to load and other conditions.

For diesel HCCI engines, the required compression ratio is typically too low for satisfactory performance of cold start and low load situations, where the temperature at the end of compression is critical and the preparation of homogeneous charge is very hard. One possible way is changing the compressed mixture temperature by using NVO. Shi et al. [11] studied the diesel HCCI combustion by directly injecting the diesel fuel into the in-cylinder residual gas during NVO interval, and found that a large amount of residual with a high temperature benefited fuel vaporization and mixing. It was concluded that increasing NVO benefited the combustion stability and fuel vaporization at low loads.

However, the influence of VVT/VVA on the in-cylinder air motion and on the interaction between air motion and the fuel spray are not yet fully understood. It is important to study various VVT/VVA operations and their effects on the behavior of in-cylinder flow field and air-fuel mixing during the induction and exhaust strokes for optimising diesel HCCI combustion performances and emissions. This will also be helpful for understanding gas dynamic effects on the engine volumetric efficiency of VVT/VVA operations. [18].

In the study described in this paper, three-dimensional CFD (Computational Fluid Dynamics) modeling was employed to simulate the gas exchange process and compression process up to top dead center (TDC) in a diesel HCCI engine with various VVT/VVA operations and early fuel injection. Firstly, the effect of NVO on gas exchange and charge preparation is discussed and then four cases with different EVO and IVC were calculated to compare the effects of the begin time and the end time of the gas exchange process on HCCI operations. Finally, three NVO strategies with different maximum valve lift and valve timing were compared to examine effects of valve lift and valve timing on retaining residual gas and control of the in-cylinder temperature, and their further influences on air motion and the mixture preparation process.

2 NUMERICAL MODEL

2.1 Methodology

The CFD code employed was KIVA-3V [19]. The turbulent flows within the combustion chamber were modeled using a modified RNG turbulence model [20]. The main modification was for variable-density engine flows. Fuel spray models were included in the code to account for spray atomization, breakup, collision, vaporization and spray/wall interaction [19]. The spray is represented by a particle method described in [19]. The interaction between the spray and the gas flow is accounted for through coupling source terms in the governing equations. Diesel fuel model DF2 (C₁₂H₂₆ Cummins model) was used in this study, which was assembled by T. L. McKinley of Cummins Engine Company. A moving-grid method was used to trace piston and valve movements.

2.2 Computational Grid

The computational domain includes intake ports and exhaust ports, the cylinder and the piston bowl, as shown in Fig. 1. Hexahedral cells were preferred for the grid generation. The number of cells varies from approximately 45,000 cells at TDC (Top Dead Centre) of compression, to 150,000 cells at BDC (Bottom Dead Centre). It has a typical grid size of 2~3 mm. Kim et al. [21] indicated that KIVA-3V results with the coarser mesh (the typical size of 2.2×2.2×3.0 mm×mm×mm) were shown with enough confidence of accuracy after comparing the results from two different mesh densities. It was observed by Juneja et al. [22] and Jia and Xie [23] that a resolution of 2 mm in the axial direction did not affect the results and the difference was less than 5% in spray vaporization simulations. For the present study, the solution obtained with the reference grids was considered sufficiently accurate.

2.3 Initial and Boundary Conditions

As this study's aim was to investigate effects of various VVT/VVA strategies on in-cylinder air motion and air-fuel mixing in a diesel HCCI engine, the simulations were conducted from BDC at the end of the expansion stroke (-180 °CA) to TDC at the end of compression stroke (360 °CA). For the descriptions in this paper, 0 °CA refers to the TDC between the exhaust stroke and the intake stroke. Initial thermodynamic and turbulence quantities were assumed to be uniform in the ports and the cylinder. In order to have a consistent reference for comparisons, the same initial and boundary conditions were used for all the computations. Constant pressure boundary conditions were assigned at inlets and outlets, so the dynamic effects were neglected in those boundary conditions. The details of the initial conditions for in-cylinder, intake port, and exhaust port regions are shown in Table 1. These values were estimated based on the low load conditions (2000 rpm and around 20% load).

3 TEST ENGINE

The test engine simulated in this paper is derived from a four cylinder high-speed direct-injection (HSDI) diesel engine with a common-rail fuel injection system. Both the cylinder bore and stroke are 86 mm, so the displacement is 0.5 litre per cylinder. The original diesel engine has a compression ratio of 18.2:1. For maintaining an ideal HCCI combustion, the compression ratio was decreased to 14.3:1 by increasing the

clearance height. The engine speed and engine load used in this study were 2000 rpm and approximately 20% respectively. The engine specifications are listed in Table 2.

For each cylinder, there are two exhaust valves and two intake valves. For two direct intake ports, inlet is tangential to the wall of the cylinder. The positions of intake ports and exhaust ports are shown in Fig. 2. The injector is located in the center of the cylinder head. Early injection was used for achieving homogeneous charge. According to the research results from Lechner et al. [24] and Kim et al. [21], a narrow cone angle nozzle with spray cone angles of 60° was employed for reducing fuel deposition on the cylinder wall. The injection parameters are listed in Table 3.

4 RESULTS AND DISCUSSIONS

4.1 The Influence of NVO

In order to explore the effects of NVO on in-cylinder flow field and mixing, four different valve profiles for obtaining different NVO have been investigated in this section. The value of NVO is defined as the crank angle difference between EVC and IVO. For all examined cases, EVO and IVC were fixed. Then the NVO value was adjusted by advancing EVC coupled to a symmetric delay of IVO. For four different valve profiles, EVC were at 0, -30, -60, -90 °CA and IVO were at 0, 30, 60 and 90 °CA respectively. This results in NVO having values of 0, 60, 120 and 180 °CA, as shown in Fig. 3. These cases are referred as NVO=0°, NVO= 60°, NVO=120° and NVO=180° in the following sections. From Fig. 3, it shows that the maximum valve lifts were changed proportionally with changed NVO.

4.1.1 Effects of NVO on Macro Properties

The graphs depicted in Fig. 4 to Fig. 6 show the in-cylinder mass, temperature and pressure with the four NVOs, respectively, and provide an understanding of the processes occurring during the gas exchange and compression strokes. In order to fully understand these results, the figures are discussed jointly.

It can be seen from Fig. 4 that more hot residual gas is trapped in the cylinder for longer NVO cases with early EVC during the exhaust stroke. Because the piston still moves up, the residual is compressed until TDC, which results in significant increments of temperature and pressure for the cases of NVO=60°, NVO=120° and NVO=180° as shown in Fig. 5 and Fig. 6. It has been found that injecting the fuel into the hot residual gas in the cylinder during the NVO interval can reform the gasoline and improve ignitability [25] and benefit the vaporization of diesel fuel [11].

As the piston starts moving down and the intake valve opens, the combustion product in the chamber flows back into the intake port and forms a small backflow because the pressure in the chamber is still higher than that in the intake ports, as shown in Fig. 5. As a result, the in-cylinder mass of residual gas has a small decrease (up to 10%) just after intake valve opening for all NVO cases, shown in Fig. 4. From this point, the IVO timing should not be totally symmetric to the EVC timing for NVO strategy, but a little delay from the symmetry point. After this backflow period, it comes into the true air induction process, and the fresh air is drawn into the combustion chamber.

Shown in Fig. 6, the temperatures at IVC (180 °CA) are 326 K, 334 K, 339 K and 342 K for NVO= 0°, NVO= 60°, NVO=120° and NVO=180° respectively. This is due to higher residual gas rate in the cylinder with higher NVO and it can be concluded that an increase of 30 °CA NVO can increase initial in-cylinder charge temperature (at IVC) of approximately 3-8 K under the operating conditions described in the above paragraphs.

Finally, the simulation results show that the amount of internal EGR rate for NVO=0° is 8%, while it is as high as 93% for NVO=180°. The total in-cylinder mass decreases slightly with longer NVO, as shown in Fig. 7. Because combustion products such as CO₂ and H₂O have a higher specific heat capacity than air, this tends to reduce compression-end temperature and causes the temperature differences with different NVO at 300 and 360 °CA to become less obvious, compared to the temperature differences at IVC, as shown in Fig. 6. It can be seen in Fig. 5 that the pressure during the compression stroke is almost the same for all NVO cases.

From comparisons of P-V diagram shown in Fig. 8, it can be seen that much residual trapped under $NVO=60^\circ$ is recompressed during the late exhaust stroke, which results in the increase of the pumping loss. Then the residual pushes the piston during the early intake stroke with late IVO. Therefore, pumping loss increases slightly for the longer NVO cases because of higher heat transfer in the recompression-expansion process.

4.1.2 Effect on In-cylinder Air Motion before Fuel Injection

In DI (Direct Injection) diesel engines, in-cylinder air motion before and during fuel injection plays a decisive role for appropriate formation of air-fuel mixture, which finally affects combustion and emissions. When operating HCCI combustion in a DI diesel engine, the presentation of in-cylinder air motion before and during fuel injection is also very critical for mixing quality and consequently HCCI combustion quality. Basically, adjusting VVT/VVA is for achieving essential residual gas rate. Under specific fuel injection pressure and timing, it will be very necessary to understand if different in-cylinder air motion and mixing resulted by different valve timing/actuation can meet the requirement of optimal HCCI combustion. In the following paragraphs, investigation and results for detailed physics in the gas exchange processes with different NVOs will be discussed.

Fig. 9 and Fig. 10 show the computed in-cylinder velocity distributions at four different crank angles with $NVO=0^\circ$ and $NVO=120^\circ$ during the exhaust stroke. The cutting plane shown in Fig. 9 is taken at the axial central cross section of the intake and exhaust port (i.e. the plane A-A shown in Fig. 2) and in Fig. 10 is the cross section of the halfway point between the piston top and the cylinder head.

It is evident that the flow trends are quite similar for both two cases, although the EVC occur at different times. The only difference is that the residual in the cylinder is continuously compressed until the piston reaches TDC for $NVO=120^\circ$. Therefore, compared to $NVO=0^\circ$, the radial velocity decreases for $NVO=120^\circ$ due to lack of the guidance of outflow as shown in Fig. 9(d), while the swirl is enhanced by preserving its angular momentum within the smaller diameter piston bowl as shown in Fig. 10(d) at $0^\circ CA$ for $NVO=120^\circ$.

The corresponding velocity fields for $NVO=0^\circ$ and $NVO=120^\circ$ during the intake stroke are shown in Fig. 11 and Fig. 12. It can be seen that both $NVO=0^\circ$ and $NVO=120^\circ$ produce a strong annular jet flow through the valve curtain area as IVO. This strong flow makes an anticlockwise swirl which is shown in Fig. 12(c). As the piston moves down, there is a significant vortex formation below the intake valve and the in-cylinder air motion is developing into a large-scale inclined tumble motion at BDC, which can be seen from Fig. 11(d).

The difference between the two cases is that the flow velocity through the intake valves during the intake process is higher with $NVO=120^\circ$ than $NVO=0^\circ$ due to reduced valve lift and the delayed IVO which makes the intake process happen under higher piston speed (see Fig. 11(c)). Therefore, there exists a larger tumbling motion in the axial plane (see Fig. 11 (d)) for $NVO=120^\circ$ compared to $NVO=0^\circ$. This is completely consistent with PIV measurements results taken by Wilson et al. [26] which provided quantitative flow characteristics of in-cylinder flows under NVO. In these PIV investigations, it was observed that NVO with reduced valve lift and duration generated intake flow velocities significantly higher than those found with typical positive overlapping valve strategies.

The computed swirl ratios are shown in Fig. 13. It can be seen that the swirl ratio decreases significantly during the exhaust stroke for $NVO=0^\circ$, but increases rapidly when the exhaust valve closes for $NVO=60^\circ$, $NVO=120^\circ$, $NVO=180^\circ$ due to the effect of compression. At around $20^\circ CA$, $NVO=0^\circ$ has the lowest swirl ratio because there is a very low piston speed and the exhaust valves have closed but the intake valves have not yet fully opened. Increased NVO results in a higher swirl ratio for the other three cases. During the intake stroke, the swirl ratio at first drops for higher NVOs, then it increases after the intake valve opens due to the induction of inflow. During the intake stroke, the maximum swirl ratios for $NVO=0^\circ$ and $NVO=60^\circ$ take place at approximately $90^\circ CA$ where the piston reaches its maximum instantaneous speed. After this, the discharge velocity from the intake port to the cylinder decreases and swirl drops slowly during the rest of the intake stroke for all cases. The reducing trend continues in the first half of compression stroke due to friction at the wall. When approaching TDC, swirl is enhanced as the flows try to preserve its angular momentum. Therefore, the last swirl ratio at the

end of compression stroke is decided by both the induction during the intake stroke and the effect of compression during the late compression stroke.

The comparisons of the tumble ratio at the x axis and tumble ratio at the y axis are shown in Fig. 14 and Fig. 15. The 'x' and 'y' are referred to the directions of x and y axes shown in Fig 2. During the exhaust stroke, the tumble ratio is generated by the exhaust flow which can be seen from Fig. 9(a), and the tumble ratio values reach the maximum just before the close of the exhaust valves. It then decreases monotonically during the latter exhaust stroke. At 0 °CA, the largest tumble ratio is predicted for the EVO=0° case. The tumble ratio during the intake stroke is well established in the whole cylinder, even in the combustion chamber for all of NVOs (see Fig. 11(c) and 11(d)). Especially for NVO=60°, strong tumble motion is generated by the air jet flow through the valve curtain areas at the early induction stage. During the following compression stroke, as the piston moves from BDC to TDC, the well-developed tumble is broken down for all of the four cases. It should be noted that the backflow taking place just after the intake valves are opened makes a short but negative contribution to the main tumble flows both at the x axis and the y axis, though this did not happen for the swirl flow.

Fig. 16 illustrates the variations of turbulence intensity for the four NVOs. It can be observed that the developments of turbulence intensity during the exhaust are similar for all cases. In contrast to NVO=0°, NVO=60° generates stronger flow fluctuation during the intake stroke due to the higher inflow velocity. However, for NVO=120° and NVO=180°, the intensity increases become smaller because the mass of fresh air induced into the cylinder is less. Before this, the backflow at the beginning of the intake process causes a short delay for the increase of the turbulence intensity. During the compression stroke, the in-cylinder flow shows very little structure and was largely piston driven upward flow without strong active generation mechanisms for turbulence kinetics energy. Therefore, turbulence intensity decreases rapidly for all NVO cases.

From Fig. 13 to Fig. 16, although swirl ratios of NVO=60° and NVO=120° are not higher than NVO=0° at the injection timing (300 °CA), their tumble ratios at x axis are much higher at the time. This means that the predicted flow fluctuations at the injection timing (300 °CA) for NVO=60° and NVO=120° are approximately

10-15% higher than $NVO=0^\circ$ (in Fig. 16). These enhanced fluctuations are especially desirable for very early direct injection and are considered beneficial for assisting the mixing process and forming enough homogeneous charge. In addition, for these two cases, the fresh air which is brought into the cylinder with high velocity during the intake stroke could also assist good mixing and combustion.

4.1.3 Effect on Air-Fuel Mixing and Temperature Distribution

In order to understand the manner of NVO's influence on mixture preparation, the air-fuel mixing process is analyzed in this section. In-cylinder velocity and temperature distributions before injection are shown in Fig. 17 to Fig. 20. From Fig. 17, it can be seen that there was stronger tumble motion at $240^\circ CA$ for $NVO=120^\circ$ than $NVO=0^\circ$. The difference in velocity distribution between these two cases becomes weaker at $300^\circ CA$, owing to the push effect when the piston keeps moving up. For swirl ratios, though in Fig. 13 it shows that $NVO=0^\circ$ has a stronger total in-cylinder swirl at $240^\circ CA$ and $300^\circ CA$ than $NVO=120^\circ$, $NVO=120^\circ$ presents a stronger swirl ratio at the halfway cross section (as shown in Fig. 18).

Fig. 19 and Fig. 20 show the temperature distributions for the two cases. It can be found that in-cylinder temperature becomes higher as NVO increases, owing to a lot of hot residual being retained in the cylinder during the exhaust stroke. More importantly, temperature distribution is more homogeneous for $NVO=120^\circ$ than $NVO=0^\circ$, which can also be seen from the typical temperature-mass distribution at $300^\circ CA$ in Fig. 21. The temperature-mass distribution gives in-cylinder mass fraction in different temperature ranges. The narrower distribution together with higher peak indicates a more homogeneous mixture. Good temperature homogeneity for $NVO=120^\circ$ should be partly contributed by higher tumble motion. However, $NVO=60^\circ$ with stronger tumble and swirl does not have a good temperature homogeneity. This suggests that there are other factors which control in-cylinder temperature homogeneity. At first, higher swirl ratio, higher tumble ratio and higher turbulence intensity should definitely be beneficial to temperature homogeneity. On the other hand, very low or very high residual gas rate will contribute temperature homogeneity too, because this will require less heat transfer between the high temperature charge and the low temperature charge. Finally, higher residual gas rate may increase temperature homogeneity due to more hot charge will reduce heat transfer from the cylinder wall to the

charge during early compression stroke when the charge has a lower temperature than the cylinder wall. Those factors working together mean NVO=120° has the highest temperature homogeneity.

Fig. 22 illustrates the droplet distribution of the fuel spray at 315 °CA, in the front and top view respectively. It was observed that there is better droplet homogeneity under similar spray penetration for NVO=120°. This demonstrates that stronger turbulence intensity and more homogeneous temperature distribution of NVO=120° help the air-fuel mixing. This is comparable to results of Jhavar and Rutland [27] who investigated the effect of engine valve actuation on mixture preparation by introducing a second intake valve opening close to the end of the compression stroke to increase air flow velocity and indicated that the droplet distribution is affected by variable valve timing, though the extent of the influence is weak compared to the traditional valve timing.

4.2 The Influence of EVO and IVC

In conventional engines, in order to make the best use of the inertia of the gases in the intake and exhaust systems for optimal volumetric efficiency, the exhaust process usually begins 40 to 60 °CA before BDC and intake valve remains open until 50 to 70 °CA after BDC [28]. When these effects of NVO were discussed in the previous section, all EVO and IVC were kept the same for a consistent reference. In this section, effects of EVO and IVC will be examined with four cases for which EVO was gradually advanced to -150, -180, -210 and -240 °CA. Corresponding with those four EVO settings, IVC was set at 150, 180, 210 and 240 °CA respectively, in order to prevent excessive back-flow of trapped residuals into the intake manifold for the early EVC, as shown in Fig. 23. For this part of the study, maximum valve lifts and valve durations of both exhaust and intake valves were kept constant. This implies there is gradually increased negative overlap between the exhaust process and intake process. Therefore, this part of the study can also be regarded as effects of NVO with same valve profiles. To differ those names used in last part, four cases described in this part are referred as EVO=-150°, EVO=-180°, EVO=-210° and EVO=-240°.

In Fig. 24 and 25, the in-cylinder mass variation and temperature histories with these four EVOs are shown. Because the exhaust valve durations are the same for all cases, earlier EVO results in less exhaust gas being

expelled from the cylinder, which can be seen from Fig. 24. As EVO is advanced from -150 to -240 °CA, the residual gas amount left in the cylinder increases. The exhaust becomes slower for advanced EVO due to a lower pressure difference between the in-cylinder and exhaust port, compared to -150 °CA EVO. Shown in Fig. 24, at the end of intake stroke, some of the in-cylinder gas flows back from the cylinder into the intake port for the case of $\text{EVO}=-240^\circ$. This is due to after 180 °CA and before IVC, the piston has started to move upward and is pushing some gas out of the cylinder. In Fig. 25, it shows that the temperatures at 180 °CA (at IVC) are 351, 370, 375 and 366 K for $\text{EVO}=-150^\circ$, $\text{EVO}=-180^\circ$, $\text{EVO}=-210^\circ$ and $\text{EVO}=-240^\circ$ respectively. Although there is the highest hot residual gas rate existing in the cylinder for $\text{EVO}=-240^\circ$, the temperature at IVC is still very low due to late IVC and high heat loss from the wall during the time between EVC and IVO.

In Fig. 26, swirl ratio, tumble ratio at x axis, tumble ratio at y axis and turbulence intensity at fuel injection timing (300 °CA) are shown for four EVOs. For these values of tumble ratios, the direction of rotation as used in Fig. 14 and Fig. 15 for demonstrating a history is neglected and just absolute values are plotted in Fig. 26 due to the tumble intensity (absolute value) is more important for practical applications. It can be found that earlier EVO produces lower swirl ratio because the induction process plays a more dominant role in the last swirl ratio. Although stronger tumble motions were once predicted during intake stroke for $\text{EVO}=-150^\circ$ and $\text{EVO}=-180^\circ$, at injection timing (300 °CA) tumble ratios have become very similar for all four cases. However, the flow fluctuations at injection timing for $\text{EVO}=-150^\circ$ and $\text{EVO}=-180^\circ$ are obviously higher than for the other two cases.

The in-cylinder mixture volume distributions with different equivalence ratio at 350°CA are shown in Fig. 27. These results actually demonstrate fuel distributions in the cylinder. Five different equivalence ratio ranges are used to evaluate the homogeneity of the fuel-air mixture. It should be noted that the global equivalence ratios are not the same for all four cases due to the different amounts of residual gas being retained in the cylinder, with the same fuel. Fig. 27 indicates that less rich fuel regions (equivalence ratios of greater than 1.5) exist in cases of $\text{EVO}=-150^\circ$ and $\text{EVO}=-180^\circ$. This is mainly due to the higher turbulence intensity and higher in-cylinder velocity which benefit the mixing processes. However, the lean mixture regions with a equivalence ratio less

than 0.0001 are slightly lower for $EVO=-150^\circ$ and $EVO=-240^\circ$ because of the lower in-cylinder pressure which leads to higher spray penetration. It can be also seen that $EVO=-150^\circ$ and $EVO=-180^\circ$ have higher volume fractions in the equivalence ratio range of 0.5 to 1.5 which is more suitable for ignition.

As far as power output is concerned, pumping losses are increased for $EVO=-210^\circ$ and $EVO=-240^\circ$ because of high heat transfer from the in-cylinder mixture to the wall in the recompression-expansion process during the NVO period. Too high advance of EVO before BDC also leads to a decrease in volumetric efficiency and power output for these two cases. For $EVO=-150^\circ$, the late EVO after BDC and early IVC before BDC result in increase of pumping work. Therefore, for the considerations to reduce pumping losses, to form a more homogeneous mixture, to increase the turbulence intensity, and to have efficient control of residual fraction and in-cylinder temperature, EVO and IVC are still kept at -180°CA and 180°CA respectively in the following section.

4.3 The Comparison of Three Different VVT/VVA Strategies

In order to trap required quantities of residual gas and control the ignition point of HCCI combustion, different VVT/VVA strategies have been studied and published. In this section, the three most popular VVT/VVA strategies shown in Fig. 3 and Fig. 28 will be compared. For these three strategies, the same baseline with 0.6 cm valve lift, exhaust process from -180°CA to 0°CA and intake process from 0°CA to 180°CA were used. The first strategy is realised by reducing the maximum valve lift from 0.6 cm to 0.3 cm while keeping the same valve timings. The corresponding cases are referred to $V_{MAX}=0.5$, $V_{MAX}=0.4$, and $V_{MAX}=0.3$ respectively, as shown in Fig. 28(a). In the second strategy, the maximum valve lift, EVO timing and IVC timing are fixed at 0.6 cm, -180°CA and 180°CA respectively. EVC timing and IVO timing are varied to retain moderate residual in the cylinder. These three cases are named as $EVC=-30^\circ$, $EVC=-60^\circ$, and $EVC=-90^\circ$, as shown in Fig. 28(b). Three cases of $NVO=60^\circ$, $NVO=120^\circ$ and $NVO=180^\circ$ in Fig. 3 are chosen as the third strategy. In order to prevent the outflow of the residual into the intake port during the intake process, IVO is symmetrically varied with EVC in all cases. The aim of comparison of these ten cases here is to investigate effects of valve lift and

valve timing on retaining residual and control of the in-cylinder temperature, and their further influences on air motion and mixture preparation process.

The variations of in-cylinder fresh air mass versus residual mass after the intake valve is closed are shown in Fig. 29 for all cases. It can be seen that VMAX strategy is not an efficient way to retain enough residual gas. But the fraction of in-cylinder air is a little more sensitive to the valve lift for VMAX strategy. On the other hand, when the adjustment of valve lift is combined with the adjustment of EVC timing, the results for controlling the residual gas rate are much more obvious than just adjusting EVC timing. These can be seen in Fig. 29, in particular between $NVO=180^\circ$ and $EVC=-90^\circ$.

In Fig. 30 the in-cylinder temperature versus residual mass at IVC is illustrated for these cases. It can be seen that, for VMAX strategy, variations on residual gas rate and in-cylinder temperature are unapparent. For in-cylinder temperature, it does not keep increasing with higher residual gas rate for reduced maximum valve lift. This may be due to the temperature increase achieved from the residual gas rate increase is less than the temperature reduction caused by higher pumping loss which results in the decrease of in-cylinder pressure and temperature. For NVO strategy and EVC strategy, there is a quick temperature change for different cases due to high variation of residual gas amount. There is also a similar trend for temperature variation versus residual gas amount for NVO and EVO strategies, though $NVO=180^\circ$ has the maximum temperature due to the maximum residual gas amount. In Fig. 30, it can also be seen that the increase in temperature gradually becomes slow when the residual mass is increased over 0.4 g.

The developments of swirl ratio for all the cases are shown in Fig. 31. For VMAX strategy, as residual fraction is increased as the maximum valve lift decreases from 0.6 to 0.3 cm, the swirl ratio at IVC decrease slightly because of low flow mass rate and low horizontal component of the inflow velocity for 0.3 cm. It can also be found from the comparisons between $EVC=-30^\circ$ and $NVO=60^\circ$, between $EVC=-60^\circ$ and $NVO=120^\circ$, as well as between $EVC=-90^\circ$ and $NVO=180^\circ$ (in each pair the valve timings are the same), there is always higher swirl

ratio at IVC for cases with higher valve lift. Hence, it can suggest that the intake flow mass rate plays a more important role than the residual motion in determining final swirl.

The tumble ratio at x axis and tumble ratio at y axis are shown in Fig. 32 and Fig. 33. As mentioned when discussing Fig. 26 in the previous section, the direction of rotation is neglected and just absolute values are plotted in these two figures. Because of original designs of intake and exhaust ports in the test engine, the tumble motion is mainly at x axis and tumble ratio at y axis is very small in all ten cases. VMAX strategy has the most obvious influence on tumble at IVC and this trend is almost kept the same at SOI (Start of Injection). For all the cases with longer intake duration, the tumble ratios at IVC are mainly controlled by the maximum valve lift. This can be testified from the variation of tumble ratio when the maximum valve lift is decreased from 0.6 to 0.3 cm in VMAX strategy. Under 0.3 cm valve lift of VMAX strategy, although less fresh air is induced into the cylinder, the higher vertical component of the inlet velocity generated by the narrower inflow area from the intake valves enhances the final tumble ratio. However, as IVO is delayed to 90 °CA in the cases of EVC=-90° and NVO=180°, the tumble ratio decreases with lowered maximum valve lift because it is more controlled by air flow mass rate. Hence, it can be concluded that the tumble ratio at IVC is mainly determined by the maximum valve lift for the cases with long intake duration. But for the cases with short intake duration, the intake valve timing becomes the critical factor.

The turbulence intensity at three different stages is shown in Fig. 34. It can be seen that the turbulence intensity trends at IVC are very similar with trends of tumble ratio at axis x. This is because the in-cylinder gas motion at 0 °CA is mainly determined by the exhaust flow. Stronger turbulence intensity can be realised from the higher inflow velocity through decreasing the maximum valve lift (e.g. VMAX=0.3), delaying IVO (e.g. EVC=-60°), or combination of these two factors (e.g. NVO=120°). Compared to tumble ratios, the turbulence intensities still keep a high value at SOI due to the dissipation of tumble motion into turbulence.

Fig. 35 shows in-cylinder mixture volume distributions with different equivalence ratio at 350°CA. All ten cases have very similar levels (approximately 36%) for the volume fraction with equivalence ratio less than 0.0001

(where there is almost no fuel in the region). Accordingly, there is approximately 64% volume being occupied by the mixture with diesel vapor. For the test engine, the volume of the combustion chamber is approximately 60% of the total in-cylinder volume at 350 °CA. Then it can be assumed that the combustion chamber is filled by the diesel vapor at the time for all cases. As the maximum valve lift is decreased or NVO is increased, the unmixed region shrinks. Then the rich fuel region expands because of the high intake velocity and high turbulence intensity. This will benefit the forming of global homogeneous charge.

In order to focus the current investigation on the influence of different VVT/VVA strategies on the mixture preparation, only one simple injection strategy was employed in this study. As the droplet distribution may be influenced more by the in-cylinder air motion caused by NVO when the average droplet size is smaller, it is recommended to explore the effects of stronger flow motion from the longer NVO on diesel HCCI mixing and combustion with advanced fuel injection strategies, such as split injection, variable geometry spray or small-hole injector. These injections normally have low injection pressure and small droplet size. These injections can be started during the induction stroke and early compression stroke, then help to form a more homogeneous fuel-air mixture.

5 CONCLUSIONS

A three-dimensional CFD modeling technical was used to investigate the effects of NVO and other VVT/VVA strategies on gas exchange processes and mixture formation processes in a diesel HCCI engine with early in-cylinder fuel injection. The following conclusions have been drawn from this study:

- Suitable NVO settings will enhance in-cylinder tumble and then increase turbulence intensity before compression-end, though the increased NVO has a negative contribution to swirl ratio.
- For NVO strategy, longer NVO will not only increase in-cylinder temperature due to higher residual gas rate, but also improve the in-cylinder temperature homogeneity. This is helpful for achieving better air-fuel mixing.
- For HCCI combustion in DI diesel engines, if considering for stronger turbulence intensity, more efficient control of residual fraction and in-cylinder temperature, lower pumping losses and more homogeneous

mixture formation, it is better to keep the EVO timing and IVC timing approximately -180 °CA and approximately 180 °CA respectively when implementing different NVO strategies.

- Among several VVT/VVA strategies, just reducing valve lifts is not an efficient way to retain the residual gas. However, combining increasing NVO and reducing valve lifts is more efficient than just increasing NVO.
- With lowering maximum valve lift or increasing NVO, the unmixed region of in-cylinder charge shrinks. The rich fuel region expands because of the high intake velocity and enhanced turbulence intensity. This is beneficial to the forming of global homogeneous charge.

ACKNOWLEDGEMENTS

The financial supports from the EPSRC and the Nuffield Foundation are gratefully acknowledged.

REFERENCES

1. Coma, G. and Gastaldi, P., *HCCI: a combustion for the future? International Journal of Vehicle Design*, Vol.41, pp2-2, 2006.
2. Atkins, M. J. and Koch, C. R., The effect of fuel octane and diluent on homogeneous charge compression ignition combustion, *Proceedings of the Institution of Mechanical Engineers, Part D: Journal of Automobile Engineering*, Vol 219, pp665-675, 2005.
3. Wang, Z., et al, Study of the Effect of Spark Ignition on Gasoline HCCI Combustion. *Proceedings of the Institution of Mechanical Engineers, Part D: Journal of Automobile Engineering*, Vol 220, pp817-825, 2006.
4. Simescu, S., Fiveland, S. B. and Dodge, L. G., An Experimental Investigation of PCCI-DI Combustion and Emissions in a Heavy-Duty Diesel Engine. *SAE paper 2003-01-0345*, 2003.
5. Strandh, P., Bengtsson, J., Johansson, R., Tunestal, P. and Johansson, B., Cycle-to-Cycle Control of a Dual-Fuel HCCI engine. *SAE paper 2004-01-0941*, 2004.

6. Yap, D., Megaritis, A. and Wyszynski, M. L., An Investigation into Bioethanol Homogeneous Charge Compression Ignition (HCCI) Engine Operation with Residual Gas Trapping, *Energy and Fuels*, Vol. 18, pp1315-1323, 2004.
7. Helmantel, A. and Denbratt, I., HCCI Operation of a Passenger Car DI Diesel Engine with an Adjustable Valve Train. *SAE Paper* 2006-01-0029, 2006.
8. Fuerhapter, A., Unger, E., Piock, W. F. and Fraidl, G. K., The New AVL CSI Engine – HCCI Operation on a Multi Cylinder Gasoline Engine. *SAE Paper* 2004-01-0551, 2004.
9. Caton, P. A., Song, H. H., Kaahaaina, N. B. and Edwards, C. F., Residual-effected homogeneous charge compression ignition with delayed intake-valve closing at elevated compression ratio. *International Journal of Engine Research*, 2005, 6(4), 399-419.
10. Murata, Y., Kawano, D., Kusaka, J., Daisho, Y., Suzuki, H., Ishii, H., Goto, Y. and Odaka, M., Achievement of Medium Engine Speed and Load Premixed Diesel Combustion with Variable Valve Timing. *SAE Paper* 2006-01-0203, 2006.
11. Shi, L., Deng, K. and Cui, Y., Study of diesel-fuelled homogeneous charge compression ignition combustion by in-cylinder early fuel injection and negative valve overlap. *Proceedings of the Institution of Mechanical Engineers, Part D: Journal of Automobile Engineering*, Vol. 219, pp1193-1201, 2005.
12. Mahrous, A. F. M., Wyszynski, M. L., Wilson, T. and Xu, H. M., Computational fluid dynamics simulation of in-cylinder flows in a motored homogeneous charge compression ignition engine cylinder with variable negative valve overlapping. *Proceedings of the Institution of Mechanical Engineers, Part D: Journal of Automobile Engineering*, Vol 221, pp1295-1304, 2007.
13. Caton, P. A., Song, H. H., Kaahaaina, N. B. and Edwards, C., Strategies for Achieving Residual-Effected Homogeneous Charge Compression Ignition Using Variable Valve. *SAE Paper* 2005-01-0165, 2005.
14. Leet, J. A., Simescu, S., Froelund, K., Dodge, L. G. and Roberts, C. E., Emissions Solutions for 2007 and 2010 Heavy-Duty Diesel Engines. *SAE Paper* 2004-01-0124, 2004.
15. Fessler, H. and Genova, M., An Electro-Hydraulic "Lost Motion" VVA System for a 3.0-Liter Diesel Engine. *SAE Paper* 2004-01-3018, 2004.

16. Nevin, R. M., Sun, Y., Gonzalez, M. A. and Reitz, R. D., PCCI Investigation Using Variable Intake Valve Closing in a Heavy Duty Diesel Engine. *SAE Paper* 2007-01-0903, 2007.
17. Kodama, Y., Nishizawa, I., Sugihara, T., Sato, N., Iijima, T. and Yoshida, T., Full-Load HCCI Operation with Variable Valve Actuation System in a Heavy-Duty Diesel Engine. *SAE Paper* 2007-01-0215, 2007.
18. Parvate-Patil, G. B. and Gordon, H. H., Analysis of Variable Valve Timing Events and Their Effects on Single Cylinder Diesel Engine. *SAE* 2004-01-2965, 2004.
19. Amsden, A. A., KIVA-3V: A Block-Structured KIVA Program for Engines with Vertical or Canted Valves. *LA-13313-MS*, 1997.
20. Han, Z. W. and Reitz, R. D., Turbulence Modeling of Internal Combustion Engines Using RNG k-e Models. *Combustion Science and Technology*, Vol.106, pp267-295, 1995.
21. Kim, M., Reitz, R. D. and Liechty, M. P., Application of Micro-Genetic Algorithms for the Optimization of Injection Strategies in a Heavy-Duty Diesel Engine. *SAE Paper* 2005-01-0219, 2005.
22. Juneja, H., Ra, Y. and Reitz, R. D., Optimization of Injection Rate Shape Using Active Control of Fuel Injection. *SAE Paper* 2004-01-0530, 2004.
23. Jia, M. and Xie, M., Numerical simulation of homogeneous charge compression ignition combustion using a multi-dimensional model, *Proceedings of the Institution of Mechanical Engineers, Part D: Journal of Automobile Engineering*, Vol 221, pp465-480, 2007.
24. Lechner, G. A., Jacobs, T., Chryssakis, C., Assanis, D. N. and Siewert, R. M., Evaluation of a Narrow Spray Cone Angle, Advanced Injection Timing Strategy to Achieve Partially Premixed Compression Ignition Combustion in a Diesel Engine. *SAE Paper* 2005-01-0167, 2005.
25. Urushihara, T., Hiraya, K., Kakuhou, A. and Itoh, T., Expansion of HCCI Operating Region by the Combination of Direct Fuel Injection, Negative Valve Overlap and Internal Fuel Reformation. *SAE Paper* 2003-01-0749, 2003.
26. Wilson, T., Haste, M., Xu, H., Richardson, S., Yap, D. and Megaritis, T., In-Cylinder Flow With Negative Valve Overlapping - Characterized By Piv Measurement. *SAE Paper* 2005-01-2131, 2005.
27. Jhavar, R. and Rutlant, C. J., Effects of Mixing on Early Injection Diesel Combustion. *SAE Paper* 2005-01-0154, 2005.

28. Heywood, J. *Internal Combustion Engine fundamentals*. McGraw-Hill, New York, 1988.

List of notation

BDC	bottom dead centre
CA	crank angle
CFD	computational fluid dynamics
CO ₂	carbon dioxide
DI	direct injection
EGR	exhaust gas recirculation
EVC	exhaust valve closing
EVO	exhaust valve opening
HC	hydrocarbon
HCCI	homogeneous charge compression ignition
HSDI	high-speed direct-injection
IVC	intake valve closing
IVO	intake valve opening
NO _x	nitrogen oxides
NVO	negative valve overlap
SI	spark ignition
SOI	start of injection
TDC	top dead centre
VMAX	maximum valve lift
VVA	variable valve actuation
VVT	variable valve timing

List of figure captions

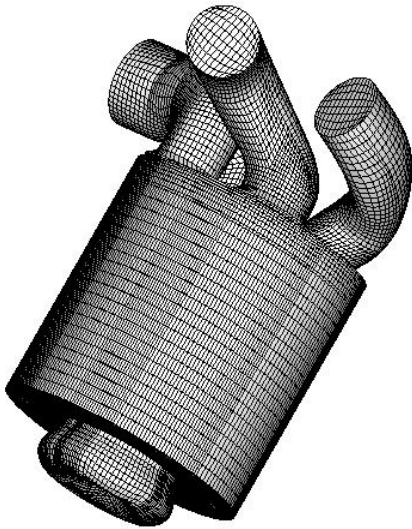


Fig. 1 Computational grids at BDC

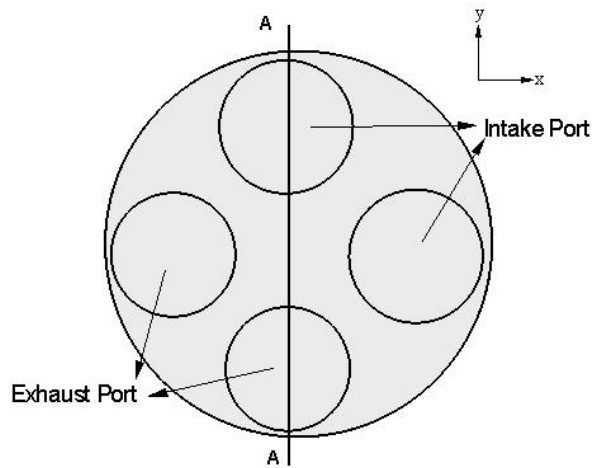


Fig. 2 Layout of the intake and outtake ports of the test engine

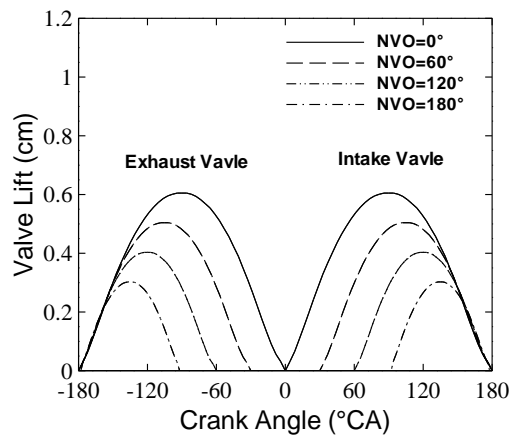


Fig. 3 Valve profiles used for simulating effects of NVO

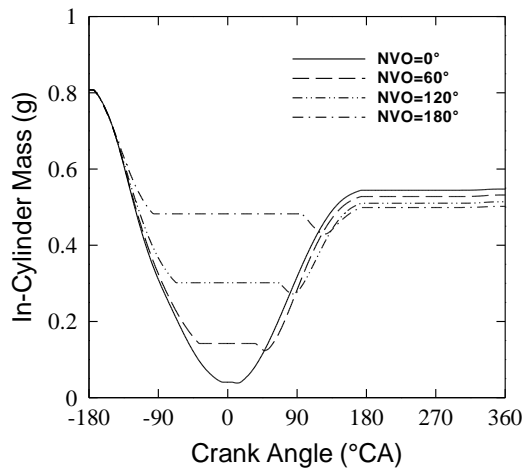


Fig. 4 In-cylinder mass as function of crank angle for different NVO

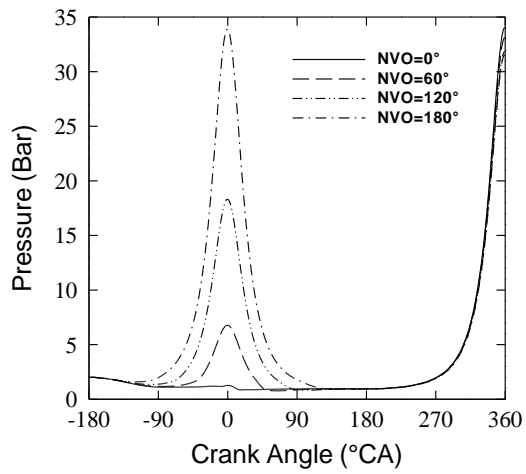


Fig. 5 Pressure as function of crank angle for different NVO

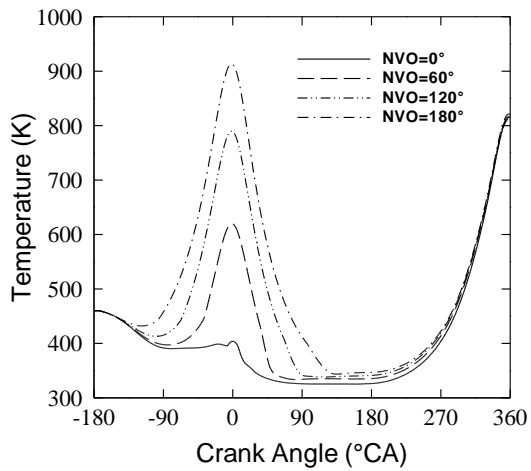


Fig. 6 Temperature as function of crank angle for different NVO

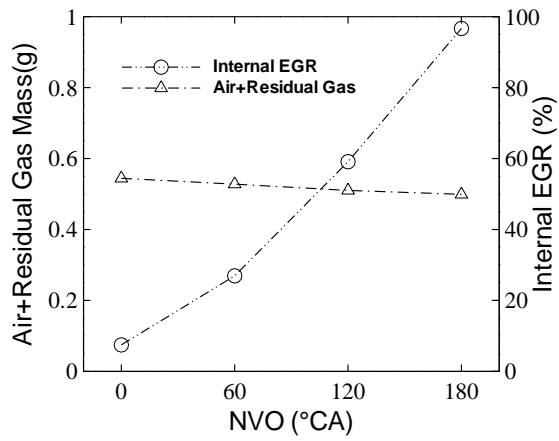


Fig. 7 Effects of NVO on the trapped residual gas rate and total in-cylinder gas at IVC

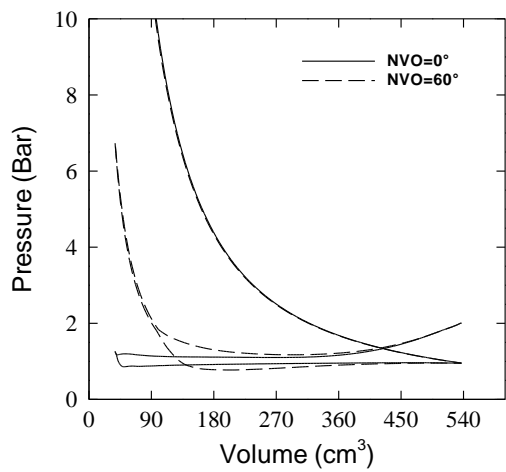


Fig. 8 P-V diagram for NVO=0° and NVO= 60°

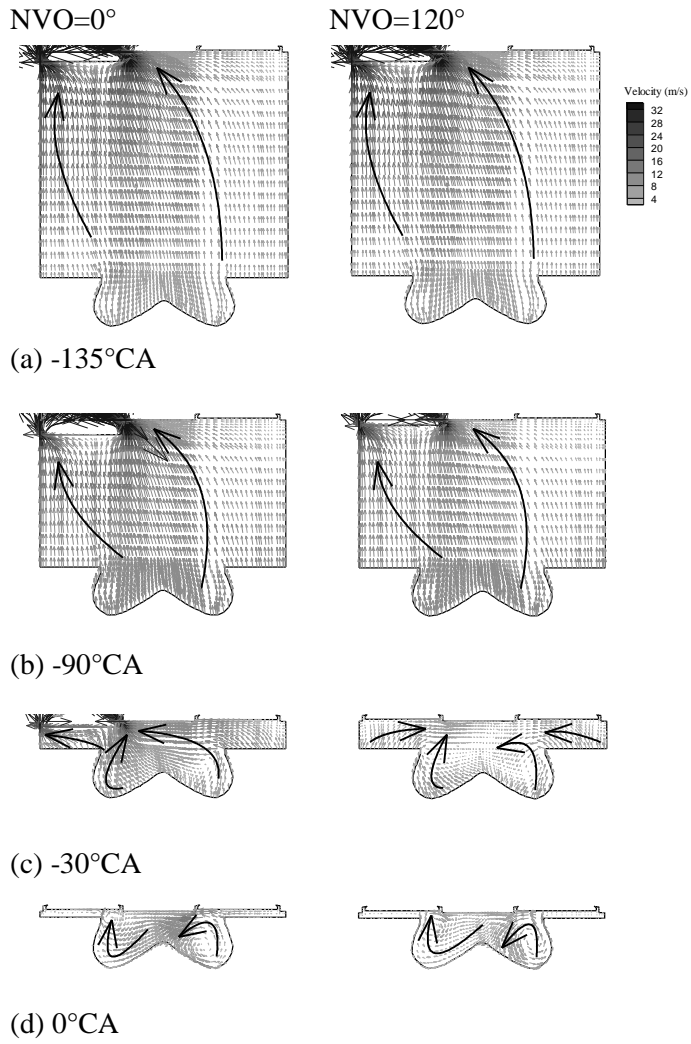


Fig. 9 Velocity distributions at axial central cross section of the intake and exhaust port during exhaust stroke

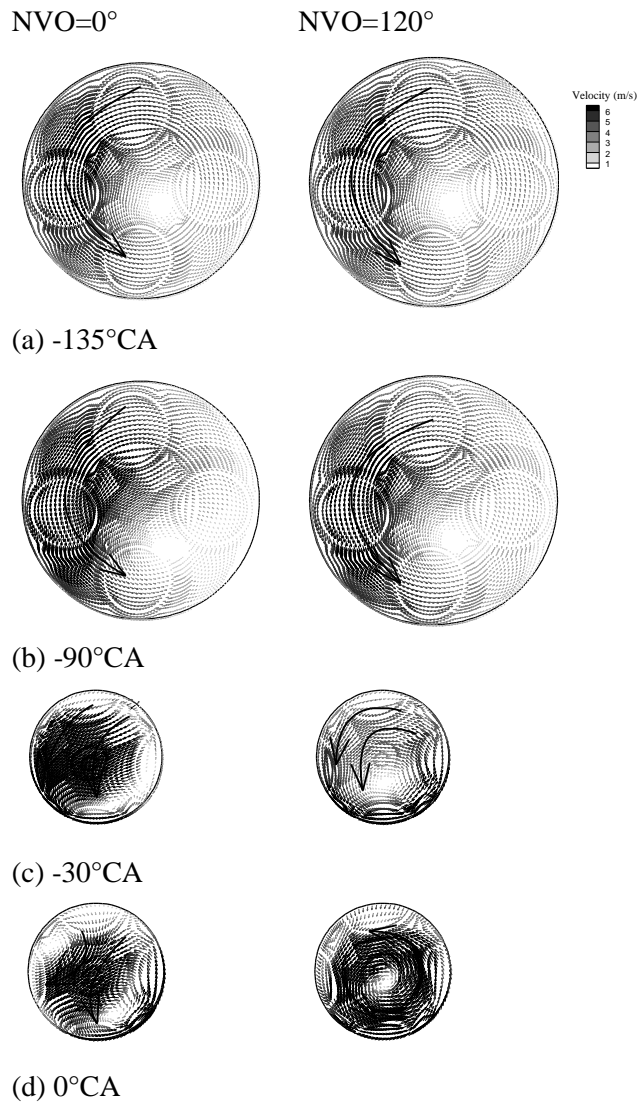


Fig. 10 Velocity distributions at the cross section of the halfway between the piston bottom and the cylinder head during exhaust stroke

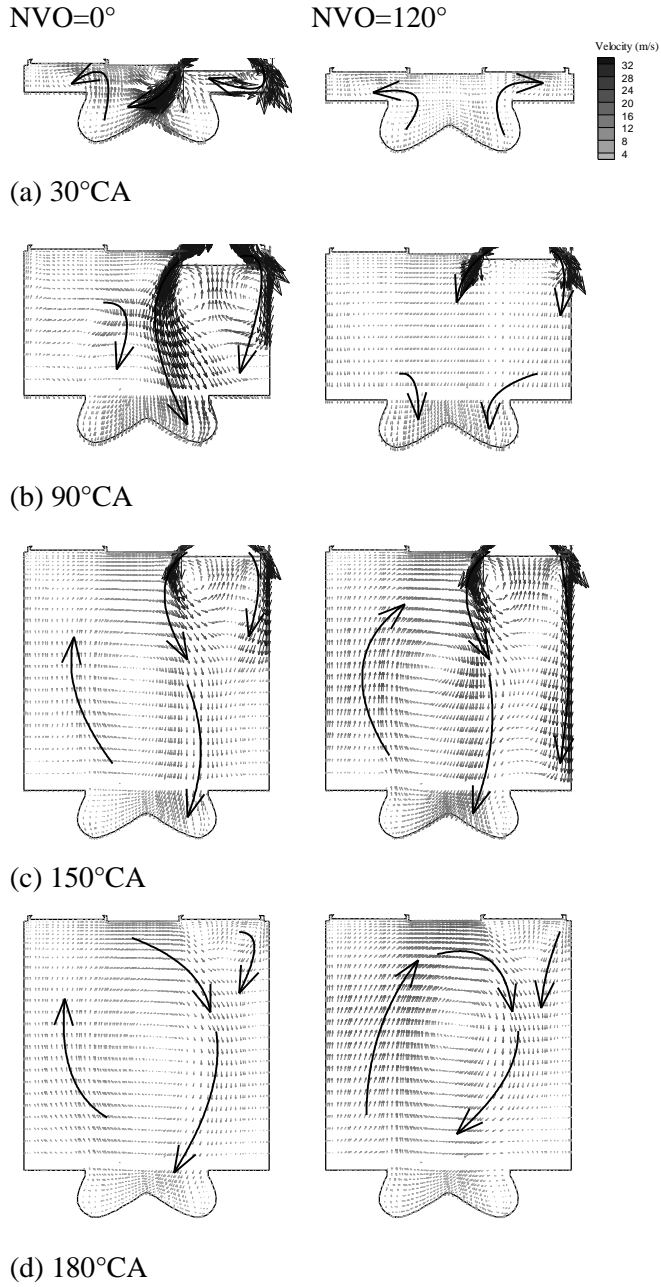
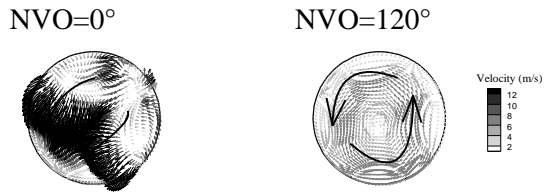
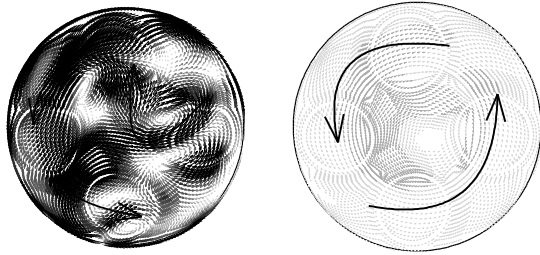


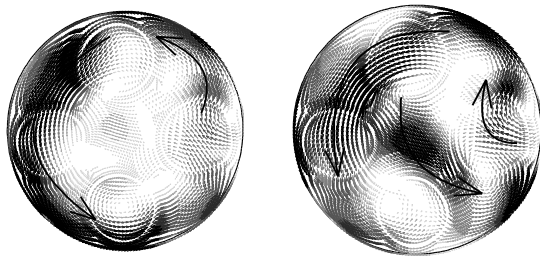
Fig. 11 Velocity distributions at axial central cross section of the intake and exhaust port during intake stroke



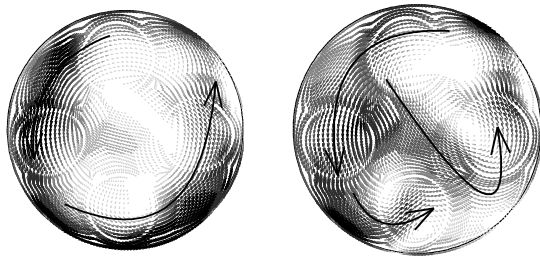
(a) 30°CA



(b) 90°CA



(c) 150°CA



(d) 180°CA

Fig. 12 Velocity distributions at the cross section of the halfway between the piston bottom and the cylinder head during intake stroke

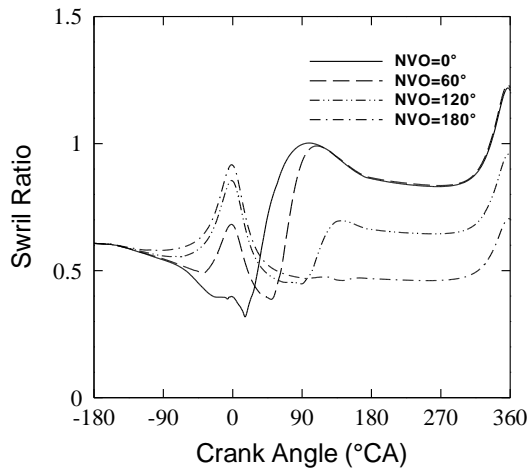


Fig. 13 Swirl ratio as function of crank angle for different NVO

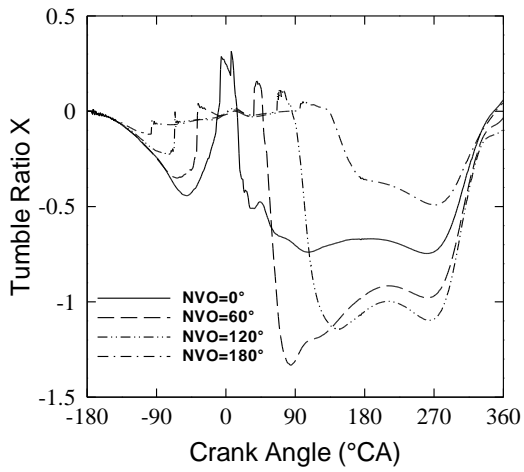


Fig. 14 Tumble ratio at x axis as function of crank angle for different NVO

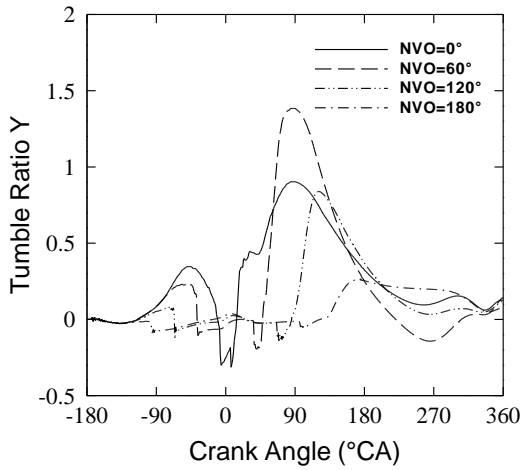


Fig. 15 Tumble ratio at y axis as function of crank angle for different NVO

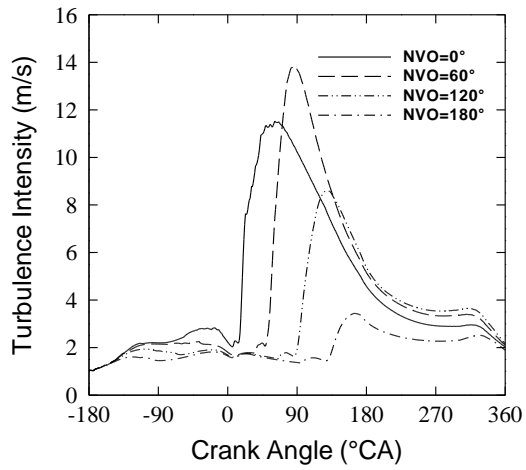


Fig. 16 Turbulence intensity as function of crank angle for different NVO

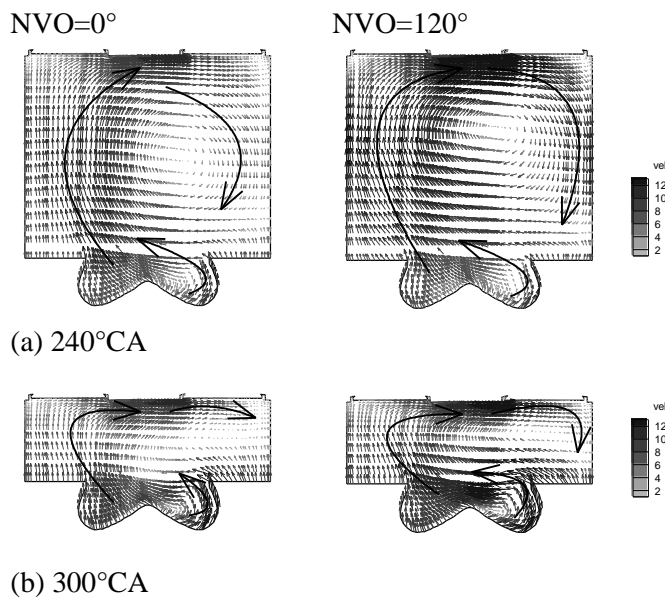
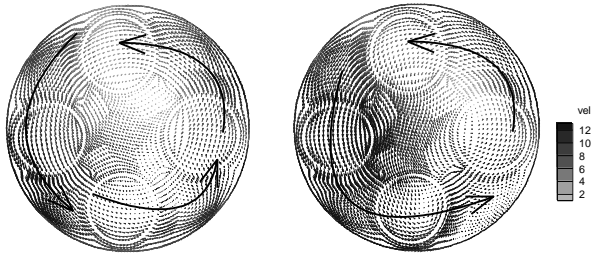


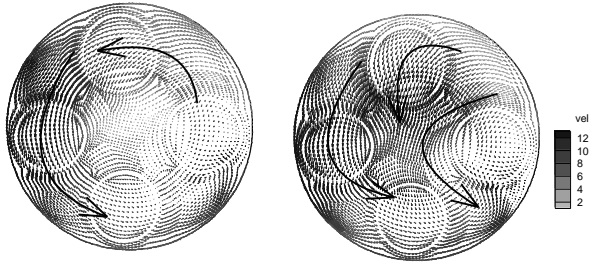
Fig. 17 Velocity distributions at axial central cross section of the intake and exhaust port during compression stroke

NVO=0°

NVO=120°



(a) 240°CA



(b) 300°CA

Fig. 18 Velocity distributions at cross section of the halfway between the piston bottom and the cylinder head during compression stroke

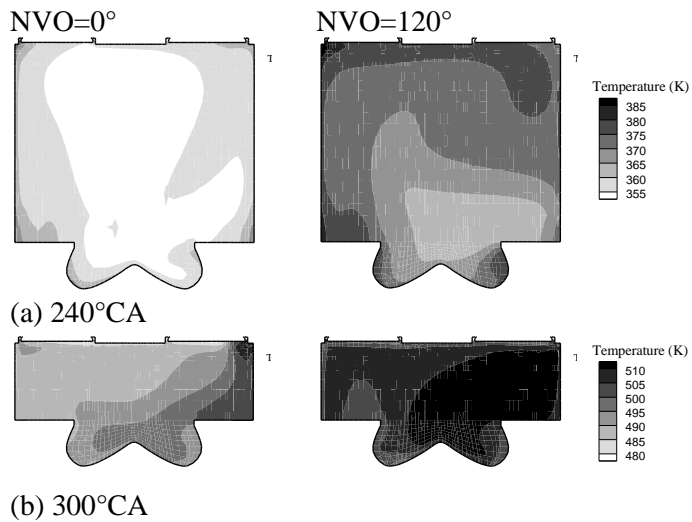


Fig. 19 Temperature distributions at axial central cross section of the intake and exhaust port during compression stroke

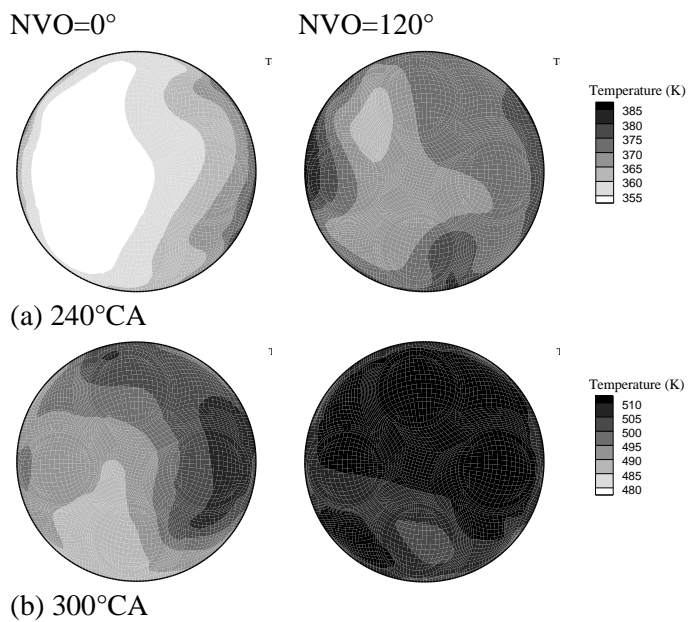


Fig. 20 Temperature distributions at cross section of the cylinder halfway between the piston and the cylinder head during compression stroke

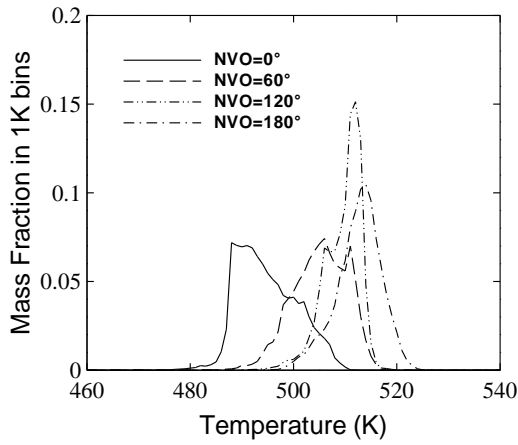


Fig. 21 Mass fraction as a function of temperature at 300°CA

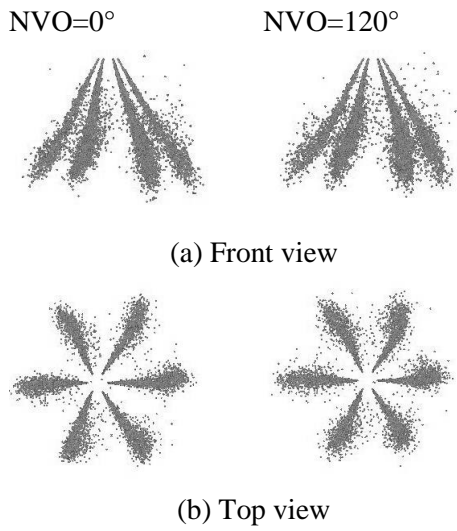


Fig. 22 Droplet distribution at 315 °CA

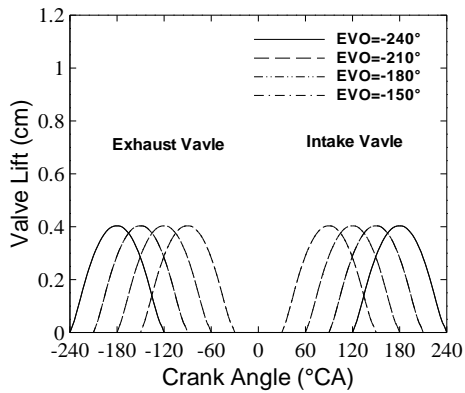


Fig. 23 Valve profiles used for simulating effects of EVO and IVC

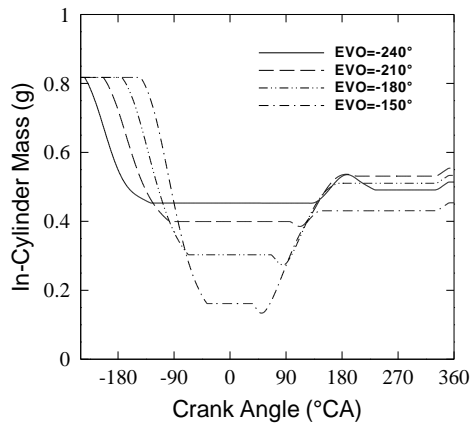


Fig. 24 In-cylinder mass as function of crank angle for different EVO

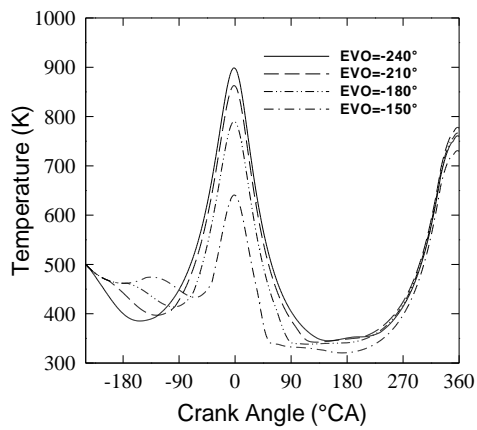


Fig. 25 Temperature as function of crank angle for different EVO

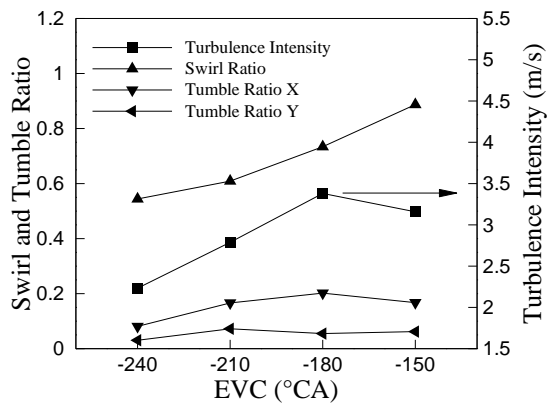


Fig. 26 Swirl ratio, tumble ratio x, tumble ratio y and turbulence intensity at 300°CA for different EVO

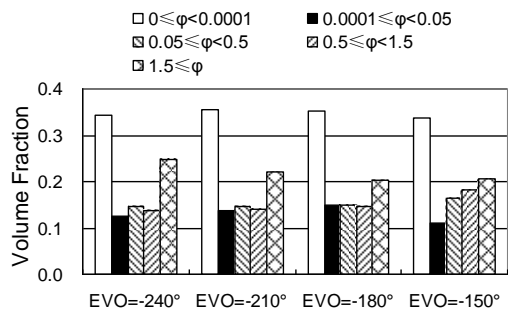
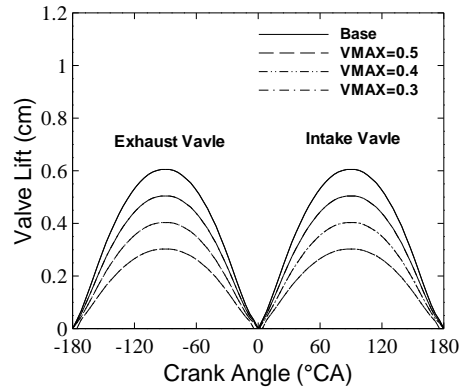
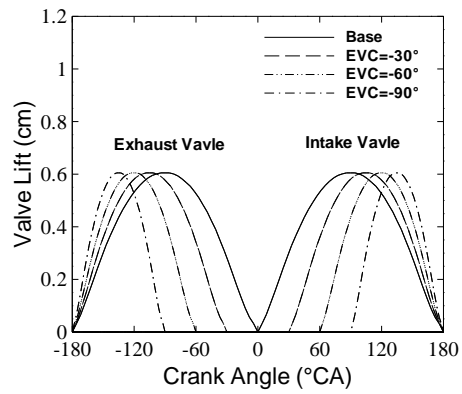


Fig. 27 In-cylinder mixture volume distributions with different equivalence ratio at 350°C



(a)



(b)

Fig. 28 Valve profiles used for different VVT/VVA strategies

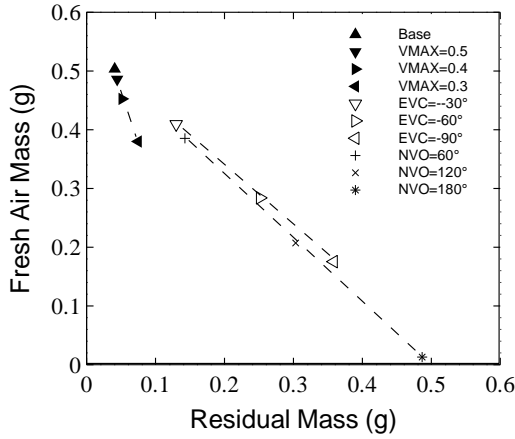


Fig. 29 Mass of fresh air versus residual mass at IVC for different VVT/VVA strategies

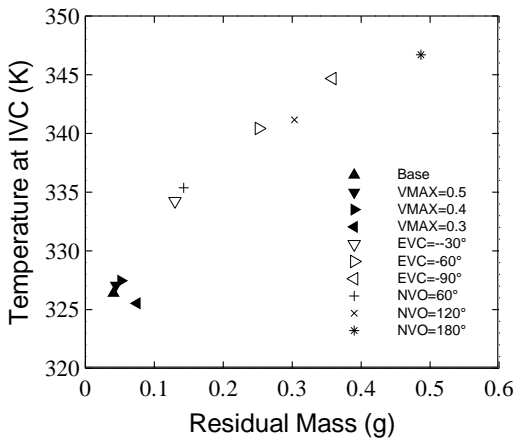


Fig. 30 In-cylinder temperature versus residual mass at IVC for different VVT/VVA strategies

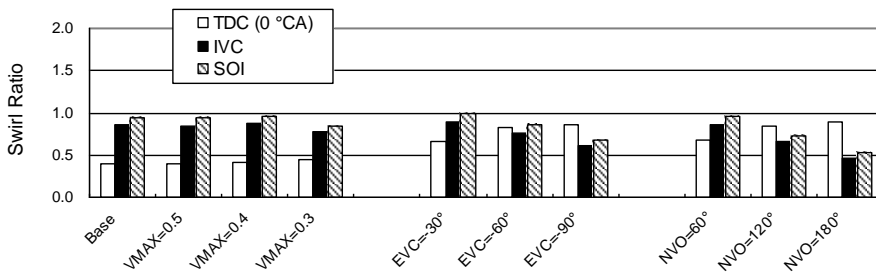


Fig. 31 Development of swirl ratio for different VVA/VVA strategies

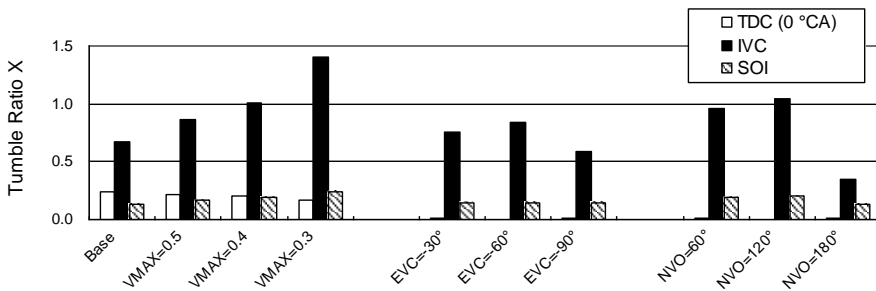


Fig. 32 Development of tumble ratio at x axis for different VVA/VVA strategies

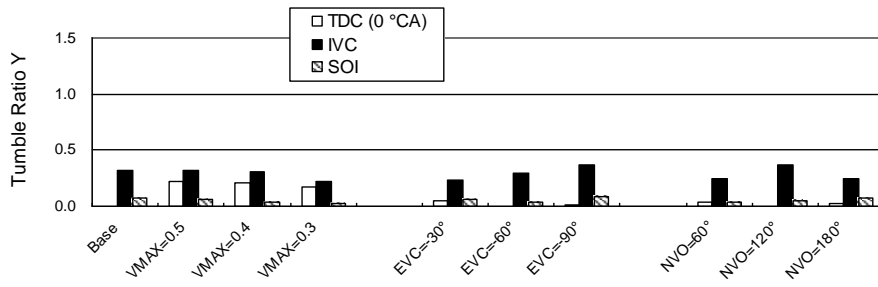


Fig. 33 Development of tumble ratio at y axis for different VVA/VVA strategies

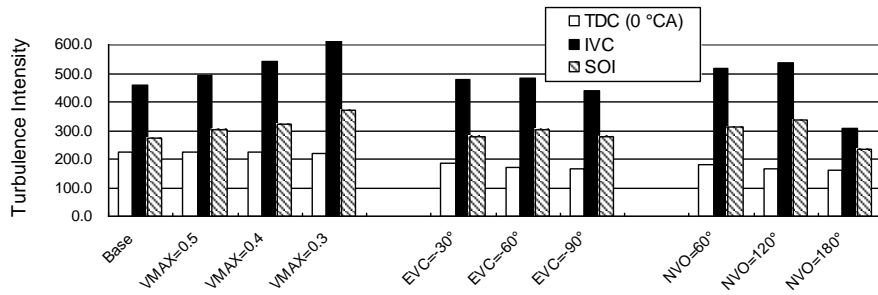


Fig. 34 Development of turbulence intensity for different VVA/VVA strategies

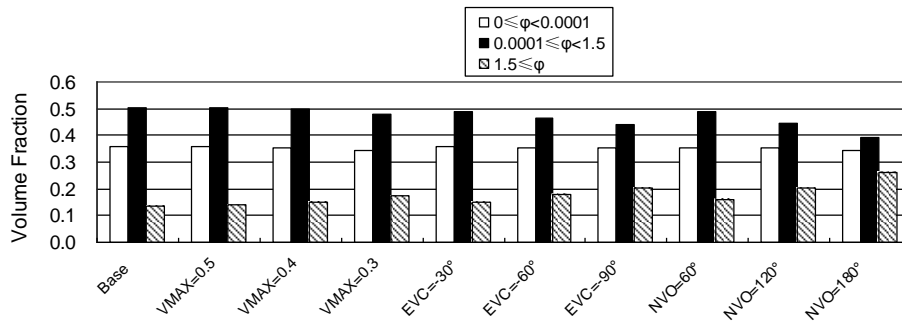


Fig. 35 In-cylinder mixture volume distributions with different equivalence ratio at 350°C

List of table captions

Table 1 Initial Conditions

	Temperature (K)	Pressure (atm)
In-Cylinder	460	2.0
Intake Port	300	1.0
Exhaust Port	480	1.0

Table 2 Engine Specifications

Displacement (single-cylinder)	0.5 L
Bore	86.0 mm
Stroke	86.0 mm
Connection Rod Length	160.0 mm
Squish Height	1.81 mm
Geometry Compression Ratio	14.3:1
Swirl Ratio	1.4
Speed	2000 rpm
Combustion Chamber	In-piston Mexican Hat
Fuel	Diesel
Wall Temperature	400 K
Firedeck Temperature	400 K
Piston Temperature	400 K

Table 3 Injection Parameters

Injector Protrusion	1.3 mm
Injector Nozzle Numbers	6
Hole Injector Diameter	0.12 mm
Injector Cone Angle	60°
Injection Timing	300 °CA (60 °CA BTDC)
Injection Pressure	300 bar
Injection Duration	2.5 ms (30 °CA)